

Density Functional Studies of 19-Electron Organometallic Complexes: Investigation of Possible Ligand Distortions and Calculation of the EPR Parameters and Unpaired Electron Distributions in $\text{CpCr}(\text{CO})_2\text{NO}^-$, $\text{CpW}(\text{NO})_2\text{P}(\text{OMe})_3$, $\text{CpMo}(\text{CO})_3\text{P}(\text{OMe})_3$, and $\text{Co}(\text{CO})_3(2,3\text{-bis(diphenylphosphino)maleic anhydride})$

Dale A. Braden and David R. Tyler*

Department of Chemistry, University of Oregon, Eugene, Oregon 97403-1253

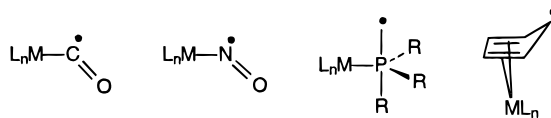
Received March 27, 2000

Density functional theory (DFT) was used to calculate the equilibrium geometries and EPR hyperfine coupling constants for the $\text{CpCr}(\text{CO})_2\text{NO}^-$ and $\text{CpW}(\text{NO})_2\text{P}(\text{OMe})_3$ 19-electron complexes. The calculated EPR hyperfine parameters for both molecules were found to be in good agreement with the experimental values. The EPR study on $\text{CpCr}(\text{CO})_2\text{NO}^-$ indicated that the nitrosyl ligand bends significantly when the neutral 18-electron parent molecule is reduced. This was confirmed by the DFT calculations, although the degree of bending is not as large as that predicted from the EPR analysis. The calculated geometry for $\text{CpW}(\text{NO})_2\text{P}(\text{OMe})_3$ showed that the nitrosyl ligands are not significantly bent, which is consistent with the crystal structure of the related compound $\text{CpW}(\text{NO})_2\text{P}(\text{OPh})_3$. In both $\text{CpCr}(\text{CO})_2\text{NO}^-$ and $\text{CpW}(\text{NO})_2\text{P}(\text{OMe})_3$, the unpaired electron is localized to about the same extent on the NO ligands. It is concluded that, although distortion of a ligand implies significant localization of the unpaired electron on that ligand, an undistorted ligand does not imply that the unpaired electron has no appreciable amplitude on that ligand. DFT was also applied to the 19-electron $\text{CpMo}(\text{CO})_3\text{P}(\text{OMe})_3$ molecule, whose role as a key intermediate in photochemical reactions of $\text{Cp}_2\text{Mo}_2(\text{CO})_6$ with $\text{P}(\text{OMe})_3$ has been inferred from mechanistic studies. It was found that loss of $\text{P}(\text{OMe})_3$ from $\text{CpMo}(\text{CO})_3\text{P}(\text{OMe})_3$ is slightly thermodynamically favorable ($\Delta E = \sim 1$ kcal/mol). This is consistent with the necessity of using an excess of the phosphorus ligand in reactions in which $\text{CpMo}(\text{CO})_3\text{PR}_3$ is believed to be the electron-transfer agent. There is no indication of $\text{P}(\text{OMe})_3$ ligand distortion in this molecule, just as there is no indication of Cp ring slippage in any of the Cp-containing molecules. Finally, a calculation of the hyperfine coupling constants in the $18 + \delta$ $\text{Co}(\text{CO})_3\text{L}_2$ ($\text{L}_2 = 2,3\text{-bis(diphenylphosphino)maleic anhydride}$) complex was also carried out. The calculated values are in reasonable agreement with experiment.

Introduction

Nineteen-electron organometallic adducts are important intermediates in many organometallic radical reactions.^{1–5} Organometallic molecules with more than 18 valence electrons are still rare, and a question of primary importance is as follows: “where” is the 19th valence electron? It has been suggested that the ligands distort in some 19-electron molecules in order to accommodate the additional electron. For example, an $\eta^5 \rightarrow \eta^4$ ring slippage, a bent CO or NO ligand, or a trigonal-

bipyramidal phosphorus ligand would convert a 19-electron structure to the presumably more stable 18-electron structure:



As part of a project to examine the electronic structure of 19-electron molecules in detail, we recently reported the results of density functional theory (DFT) calculations on $\text{CpCo}(\text{CO})_2^-$ and $\text{Mn}(\text{CO})_5\text{Cl}^-$.^{6,7} The calculations found that in both molecules the 19th electron was delocalized over the entire molecule and there were no ligand distortions in either molecule. EPR measurements likewise found no evidence of ligand distortion in these molecules.^{6,7}

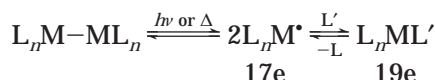
Herein we report the results of DFT calculations on 4 additional 19-electron molecules, with a particular

- (1) Astruc, D. *Chem. Rev.* **1988**, *88*, 1189–1216.
- (2) Tyler, D. R. In *Organometallic Radical Processes*; Troglor, W. C., Ed.; Elsevier: New York, 1990; pp 338–364.
- (3) Tyler, D. R.; Mao, F. *Coord. Chem. Rev.* **1990**, *97*, 119.
- (4) Tyler, D. R. *Acc. Chem. Res.* **1991**, *24*, 325–331.
- (5) Geiger, W. E. *Acc. Chem. Res.* **1995**, *28*, 351–357.
- (6) Braden, D. A.; Tyler, D. R. *J. Am. Chem. Soc.* **1998**, *120*, 942–947.
- (7) Braden, D. A.; Tyler, D. R. *Organometallics* **1998**, *17*, 4060–4064.

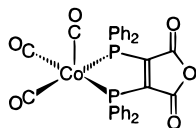
emphasis on looking at the role of ligand distortions in accommodating the "extra" electron. One of the molecules is $\text{CpCr}(\text{CO})_2\text{NO}^-$.⁸ EPR studies have shown that the M–N–O bond angle in 18-electron nitrosyl complexes bends after 1-electron reduction, and $\text{CpCr}(\text{CO})_2\text{NO}^-$ was studied therefore to see if DFT could predict the observed bending of the nitrosyl ligand. In contrast, it is known from a crystal structure that the NO ligands in $\text{CpW}(\text{NO})_2\text{P}(\text{OPh})_3$ do not bend significantly. (The W–N–O angles are 166 and 175°.)⁹ These bond angles are comparable to those in many 18-electron metal nitrosyl complexes, and their nonlinearity can be ascribed to crystal packing forces (see Results and Discussion). To see if DFT could successfully model this 19-electron compound, the phenyl groups were replaced by methyl groups so that a full geometry optimization was feasible.

The third molecule examined was $\text{CpMo}(\text{CO})_3\text{P}(\text{OMe})_3$, a reactive intermediate formed in the photolysis of $\text{Cp}_2\text{Mo}_2(\text{CO})_6$ in the presence of an excess of $\text{P}(\text{OMe})_3$ (Scheme 1).¹⁰ There is some speculation that the phosphorus ligand in this and related molecules may distort to a trigonal-bipyramidal geometry so as to accommodate the unpaired electron. Because these short-lived adducts are difficult to observe spectroscopically, we carried out DFT calculations on $\text{CpMo}(\text{CO})_3\text{P}(\text{OMe})_3$ to see if the phosphite ligand does in fact distort to a trigonal-bipyramidal geometry. The calculation was also used to determine whether this molecule is stable to dissociation of $\text{P}(\text{OMe})_3$.

Scheme 1



Finally, to test the ability of DFT to reproduce as many experimental variables as possible for a wide variety of 19-electron complexes, we report the results of a calculation on $\text{Co}(\text{CO})_3\text{L}_2$ ($\text{L}_2 = 2,3\text{-bis}(\text{diphenylphosphino})\text{maleic anhydride}$),¹¹ a special type of 19-electron molecule known as an $18 + \delta$ complex:



(These molecules are ligand-localized 19-electron complexes, i.e., 18-electron molecules with a reduced ligand. δ represents the amount of the unpaired electron's charge on the metal.⁴) EPR studies of this molecule suggested that the unpaired electron was localized primarily in the maleic anhydride ring with a spin density of only 0.02 on the cobalt atom.^{12–14} This was

supported by a subsequent $\text{X}\alpha$ calculation in which the phenyl rings were substituted with hydrogens.¹⁴ We carried out hybrid-DFT calculations on this molecule but retained the phenyl rings in order to preserve the full electronic structure of the molecule.

Computational Methods

All calculations were carried out with Gaussian 98¹⁵ using a spin-unrestricted orbital formalism. The geometries and molecular properties of all molecules were calculated using the B3LYP hybrid density functional, as defined in Gaussian 98,^{16,17} and the BP86 functional.^{18,19} The Stuttgart small-core pseudopotentials and recommended basis sets (31111/44111/411 contraction)²⁰ were used for Mo and W (28 and 60 core electrons, respectively),²¹

and Ahlrichs' all-electron TZV basis sets were used for all other atoms, including Cr and Co.²² Two p polarization functions were added for Cr and Co, with exponents equal to those for the two most diffuse s functions. Addition of diffuse functions to the basis sets for the $\text{CpCr}(\text{CO})_2\text{NO}^-$ anion did not significantly change the calculated EPR parameters. Both isotropic hyperfine coupling (hfc) constants, A_{iso} , and anisotropic hfc constants, T_{ii} , were calculated (the latter are available in Gaussian 98 using the Prop=EPR option). Further details are available elsewhere.^{6,23} The geometry of $\text{CpCr}(\text{CO})_2\text{NO}^-$ was fully optimized under C_s symmetry using both density functionals. The geometries of $\text{CpW}(\text{NO})_2\text{P}(\text{OMe})_3$ and $\text{CpMo}(\text{CO})_3\text{P}(\text{OMe})_3$ were optimized using B3LYP without any symmetry constraints, as is indicated by the crystal structure of $\text{CpW}(\text{NO})_2\text{P}(\text{OPh})_3$. A single-point energy calculation on $\text{CpW}(\text{NO})_2\text{P}(\text{OMe})_3$ was also performed using the BP86 functional. Only a single-point energy calculation using the B3LYP functional was carried out on $\text{Co}(\text{CO})_3\text{L}_2$, because this allowed the inclusion of the four phenyl rings in the L_2 ligand. (The molecule was too large for a full geometry optimization.) The molecular geometry employed was that of the crystal structure,⁸ and the wave function was constrained to C_s symmetry.

Results and Discussion

Geometries. In the optimized calculated structures of $\text{CpCr}(\text{CO})_2\text{NO}^-$, $\text{CpW}(\text{NO})_2\text{P}(\text{OMe})_3$, and $\text{CpMo}(\text{CO})_3\text{P}$ –

(15) Frisch, M. J.; Trucks, G. W.; Schlegel, H. B.; Scuseria, G. E.; Robb, M. A.; Cheeseman, J. R.; Zakrzewski, V. G.; Montgomery, J. A., Jr.; Stratmann, R. E.; Burant, J. C.; Dapprich, S.; Millam, J. M.; Daniels, A. D.; Kudin, K. N.; Strain, M. C.; Farkas, O.; Tomasi, J.; Barone, V.; Cossi, M.; Cammi, R.; Mennucci, B.; Pomelli, C.; Adamo, C.; Clifford, S.; Ochterski, J.; Petersson, G. A.; Ayala, P. Y.; Cui, Q.; Morokuma, K.; Malick, D. K.; Rabuck, A. D.; Raghavachari, K.; Foresman, J. B.; Cioslowski, J.; Ortiz, J. V.; Stefanov, B. B.; Liu, G.; Liashenko, A.; Piskorz, P.; Komaromi, I.; Gomperts, R.; Martin, R. L.; Fox, D. J.; Keith, T.; Al-Laham, M. A.; Peng, C. Y.; Nanayakkara, A.; Gonzalez, C.; Challacombe, M.; Gill, P. M. W.; Johnson, B. B.; Chen, W.; Wong, M. W.; Andres, J. L.; Gonzalez, C.; Head-Gordon, M.; Replogle, E. S.; Pople, J. A. *Gaussian 98, Revision A.4*; Gaussian, Inc., Pittsburgh, PA, 1998.

(16) Becke, A. D. *J. Chem. Phys.* **1993**, *98*, 5648–5652.

(17) Stephens, P. J.; Devlin, F. J.; Chabalowski, C. F.; Frisch, M. J. *J. Phys. Chem.* **1994**, *98*, 11623–11627.

(18) Becke, A. D. *Phys. Rev. A* **1988**, *38*, 3098.

(19) Perdew, J. P. *Phys. Rev. B* **1986**, *33*, 8822–8824.

(20) Andrae, D.; Haeussermann, U.; Dolg, M.; Stoll, H.; Preuss, H. *Theor. Chim. Acta* **1990**, *77*, 123–141.

(21) Basis sets were obtained from the Extensible Computational Chemistry Environment Basis Set Database, Version 1.0, as developed and distributed by the Molecular Science Computing Facility, Environmental and Molecular Sciences Laboratory, which is part of the Pacific Northwest Laboratory, P.O. Box 999, Richland, WA 99352, and funded by the U.S. Department of Energy. The Pacific Northwest Laboratory is a multiprogram laboratory operated by Battelle Memorial Institute for the U.S. Department of Energy under Contract DE-AC06-76RLO 1830. Contact David Feller, Karen Schuchardt, or Don Jones for further information.

(22) Schäfer, A.; Huber, C.; Ahlrichs, R. *J. Chem. Phys.* **1994**, *100*, 5829–5835.

(23) Wetmore, S. D.; Boyd, R. J.; Eriksson, L. A. *J. Chem. Phys.* **1997**, *106*, 7738–7748.

(8) Geiger, W. E.; Rieger, P. H.; Tulyathan, B.; Rausch, M. D. *J. Am. Chem. Soc.* **1984**, *106*, 7000–7006.

(9) Yu, Y. S.; Jacobson, R. A.; Angelici, R. J. *Inorg. Chem.* **1982**, *21*, 3106–3110.

(10) Philbin, C. E.; Goldman, A. S.; Tyler, D. R. *Inorg. Chem.* **1986**, *25*, 4434–4436.

(11) Fenske, D. *Chem. Ber.* **1979**, *112*, 363–375.

(12) Mao, F.; Tyler, D. R.; Keszler, D. *J. Am. Chem. Soc.* **1989**, *111*, 130–134.

(13) Mao, F.; Tyler, D. R.; Rieger, A. L.; Rieger, P. H. *J. Chem. Soc., Faraday Trans.* **1991**, *87*, 3113–3119.

(14) Mao, F.; Tyler, D. R.; Bruce, M. R. M.; Bruce, A. E.; Rieger, A. L.; Rieger, P. H. *J. Am. Chem. Soc.* **1992**, *114*, 6418–6424.

Table 1. Observed and Calculated EPR Data for $\text{CpCr}(\text{CO})_2\text{NO}^-$, $\text{CpW}(\text{NO})_2\text{P}(\text{OMe})_3$, and $\text{Co}(\text{CO})_3\text{L}_2^a$

EPR Data										
CpCr(CO) ₂ NO [−]				CpW(NO) ₂ P(OMe) ₃				Co(CO) ₃ L ₂		
	exptl ^b	BP86 ^b	B3LYP ^b		exptl ^c	BP86 ^c	B3LYP ^c		exptl ^{c,d}	B3LYP ^c
A _{iso} (N)	11.3 ± 0.2	6.6	9.3	A _{iso} (N)	7.0	1.8	5.4	A _{iso} (P)	(−)11.98	−13.0
T _{zz} (N)	13.2 ± 0.5 (T)	12.4	15.8	A _{iso} (P)	~4.7 ^e	2.5	6.5	A _{iso} (Co)	~(−)1.4	4.8
T _{yy} (N)	−6.6 ± 0.5 (T _⊥)	−6.5	−9.8					T _{zz} (Co)	(−)2.8 (T)	−8.3
T _{xx} (N)	−6.6 ± 0.5 (T _⊥)	−5.8	−6.0					T _{yy} (Co)	~1.4 (T _⊥)	4.6
								T _{xx} (Co)	~1.4 (T _⊥)	3.6
SOMO Composition (%)										
CpCr(CO) ₂ NO [−]				CpW(NO) ₂ P(OMe) ₃				Co(CO) ₃ L ₂		
	exptl	BP86	B3LYP		BP86	B3LYP				BP86
Cr		30	31	W	7	6	Co			1
Cr (s)		5	5	W (s)	0	0	Co (s)			0
Cr (p)		6	6	W (p)	7	6	Co (p)			0
Cr (d)		19	20	W (d)	0	0	Co (d)			1
Cp		23	22	Cp	32	32	CO			0
N	~40	23	25	N	32	33	PPh ₂			37
O		15	15	O	28	28	maleic anhydride			61
CO		8	7	P(OMe) ₃	1	1				

^a Units of hyperfine coupling are given in units of 10^{-4} cm^{-1} . Experimental EPR data for $\text{CpW}(\text{NO})_2\text{P}(\text{OMe})_3$ are interpolated from $\text{CpW}(\text{NO})_2\text{P}(\text{OPh})_3$ and $\text{CpW}(\text{NO})_2\text{PPh}_3$. The signs for the total hyperfine tensor elements were not determined experimentally. The calculated signs are used here, but see the text for the case of $\text{Co}(\text{CO})_3\text{L}_2$. ^b In frozen DMF at 223 K; units are 10^{-4} cm^{-1} . ^c In gauss. ^d In toluene at 115 K. ^e Average of 5.0 G observed for $\text{CpW}(\text{NO})_2\text{P}(\text{OPh})_3$ and 4.4 G observed for $\text{CpW}(\text{NO})_2\text{PPh}_3$ in acetone solution at 245 K.

(OMe)₃, the Cp rings are planar and essentially normal to the metal–centroid axis, and the calculated M–C distances are uniform.²⁴ Similar results were obtained in a prior calculation on the $\text{CpCo}(\text{CO})_2^-$ anion.⁶ These results indicate that the Cp ring tends to retain its η^5 coordination to the metal in these types of 19-electron complexes. The phosphite ligands in $\text{CpW}(\text{NO})_2\text{P}(\text{OMe})_3$ and $\text{CpMo}(\text{CO})_3\text{P}(\text{OMe})_3$ were calculated to have a tetrahedral geometry, even though the optimizations allowed for a distortion to a trigonal-bipyramidal-based geometry. The lack of distortion is consistent with the fact that the SOMO is not localized at all on the phosphite ligand in either molecule (see below). The Mo–C–O angles in $\text{CpMo}(\text{CO})_3\text{P}(\text{OMe})_3$ were calculated to be 169, 170, and 178°. The slight bending of the first two Mo–C–O bond angles indicates that the unpaired electron is partially occupying one of the p orbitals on the carbon atoms. The Cr–C–O angles in $\text{CpCr}(\text{CO})_2\text{NO}^-$ were 179°, as calculated using both density functionals. The W–N–O angles in $\text{CpW}(\text{NO})_2\text{P}(\text{OMe})_3$ were 174 and 175°. In general, there is little distortion of the ligands in these molecules, due to the presence of the 19th valence electron, except for the bending of the nitrosyl ligand in $\text{CpCr}(\text{CO})_2\text{NO}^-$ (Cr–N–O angle 157°), which is significant. The primary structural change in all three molecules is the expected lengthening of the metal–ligand bonds due to the occupation of a mostly antibonding molecular orbital (see below).

In the EPR analysis of $\text{CpCr}(\text{CO})_2\text{NO}^-$, the Cr–N–O bond angle was related to the p:s hybridization ratio on N, which was stated to be about 10.⁸ This led to a predicted Cr–N–O angle of <130°. The Cr–N–O bond angle calculated by DFT is 157°. This is significantly bent compared to the Cr–N–O angle in the 18-electron parent molecule, which is ~179° in the crystal²⁵ and 177° as calculated by DFT.²⁶ In the other 19-electron nitrosyl complex, $\text{CpW}(\text{NO})_2\text{P}(\text{OMe})_3$, the two W–N–O

angles (174, 175°) are not significantly bent according to DFT calculations or according to the crystal structure of $\text{CpW}(\text{NO})_2\text{P}(\text{OPh})_3$ (166, 175°).¹⁰ In the crystal structure of the closely related 18-electron complex $\text{CpW}(\text{NO})_2\text{Cl}$, the W–N–O angles are 168 and 169°, respectively,⁹ which shows that the slight bending of the W–N–O angles in $\text{CpW}(\text{NO})_2\text{P}(\text{OMe})_3$ and $\text{CpW}(\text{NO})_2\text{P}(\text{OPh})_3$ is not necessarily due to the unpaired electron. From these results it is concluded that DFT is capable of accurately reproducing the experimentally observed geometries for these 19-electron complexes, regardless of whether the ligands distort.

EPR Hyperfine Coupling Constants. Table 1 contains the calculated and experimental hfc constants of $\text{CpCr}(\text{CO})_2\text{NO}^-$ and $\text{CpW}(\text{NO})_2\text{P}(\text{OMe})_3$. The $\text{CpCr}(\text{CO})_2\text{NO}^-$ anion has at most a mirror plane of symmetry, but in the EPR analysis, as is common, it was assumed to possess a C_3 axis of symmetry so that its hyperfine tensor could be treated as axial.⁸ This assumption reduces the number of unique tensor eigenvalues from 3 to 2, and it simplifies fitting of the EPR spectrum and relating the results to the geometry and electronic structure of the molecule. Calculated hfc constants are based on the actual molecular symmetry; therefore, in Table 1 the degenerate experimental value for T_{\perp} is to be compared with the two calculated values T_{yy} and T_{xx} or with their average. The isotropic hfc constants for N and P in $\text{CpW}(\text{NO})_2\text{P}(\text{OPh})_3$ and $\text{CpW}(\text{NO})_2\text{PPh}_3$ have been reported, along with their reduction potentials and IR spectra.⁹ No hfc was determined for $\text{CpW}(\text{NO})_2\text{P}(\text{OMe})_3$ because it decomposed before an EPR analysis could be performed. In Table 1, the range of A_{iso} values for $\text{CpW}(\text{NO})_2\text{P}(\text{OMe})_3$ is actually that reported for $\text{CpW}(\text{NO})_2\text{P}(\text{OPh})_3$ and $\text{CpW}(\text{NO})_2\text{PPh}_3$. Because the hfc constants for these two compounds are identical for N

(24) The range of M–C bond lengths was 0.052 Å for $\text{CpCr}(\text{CO})_2\text{NO}^-$ calculated using B3LYP and 0.060 Å using BP86, 0.033 Å for $\text{CpW}(\text{NO})_2\text{P}(\text{OMe})_3$, and 0.154 Å for $\text{CpMo}(\text{CO})_3\text{P}(\text{OMe})_3$.

(25) Atwood, J. L.; Shakir, R.; Malito, J. T.; Herberhold, M.; Kremnitz, W.; Bernhagen, W. P. E.; Alt, H. G. *J. Organomet. Chem.* **1979**, *165*, 65–78.

(26) This result was obtained from an optimization using the B3LYP functional and the same basis set as was used for the 19-electron complex.

and nearly so for P, the hfc that would be observed for $\text{CpW}(\text{NO})_2\text{P}(\text{OMe})_3$ is expected to be very similar.

No hyperfine coupling to Cr was observed in the $\text{CpCr}(\text{CO})_2\text{NO}^-$ anion, and the upper bound on its magnitude was reported to be 6 G.⁸ The calculated isotropic coupling using the B3LYP functional is only -1.8 G (-1.7 G using BP86), and the anisotropic coupling constants are 5.1, -3.8 , and -1.3 G (4.6, -3.7 , and -0.9 G using BP86), which is completely within the experimental upper bound.

Table 1 shows that the hfc constants calculated using the BP86 functional are smaller in magnitude than those calculated using the B3LYP functional and also smaller than the experimental values. This behavior has been observed before.^{27,28} Overall, B3LYP gives slightly better results and they are in good agreement with the experimental values.

For $\text{Co}(\text{CO})_3\text{L}_2$, the hyperfine coupling was observed to increase with decreasing temperature for P and to decrease with decreasing temperature for Co.^{13,29} The lowest temperature at which EPR data were acquired was 115 K. At this temperature, the coupling to the phosphorus nuclei was still isotropic, and the coupling to the cobalt nucleus was treated as axial. A pronounced solvent dependence was also observed.¹⁴ For these reasons and because the molecular geometry was not optimized in our calculations, the calculated hyperfine parameters are not expected to agree as closely with the experimental values as was the case for $\text{CpCr}(\text{CO})_2\text{NO}^-$. The observed hfc values for $\text{Co}(\text{CO})_3\text{L}_2$ in toluene were chosen for comparison to the calculated values because toluene was the least polar solvent employed in the EPR studies. Table 1 shows that the observed isotropic hfc for P is actually well reproduced by the DFT calculations. Using the reported value for the dependence of the phosphorus hfc on temperature,¹³ a linear extrapolation to 0 K resulted in a value of about -13.2 G. This value agrees very well with the calculated value of -13.0 G. The observed total hyperfine coupling to cobalt was very small (4.23 G), and the perpendicular components were too small to determine accurately. (They were reported to be less than 0.4 G.) The signs of the hfc were not determined, and those used in Table 1 were arbitrarily chosen to match the calculated signs for the anisotropic coupling. The agreement between the observed and calculated values is acceptable, considering the sensitivity of the hfc of $\text{Co}(\text{CO})_3\text{L}_2$ to temperature and to environmental effects.

The calculated hfc constants are close to the observed values for all four molecules, and it is reasonable to assume, therefore, that the spin density in these molecules is adequately modeled by the DFT-MO method. We now examine the orbital in each of these 19-electron complexes that corresponds to the formally unpaired electron in order to answer the question posed in the Introduction: namely, "where" is the 19th electron? Some prefatory comments are in order. We will refer to the orbital corresponding to the unpaired electron as the SOMO, "singly occupied molecular orbital". In a

spin-unrestricted MO formalism such as the one we have used here, all orbitals are, strictly speaking, singly occupied. However, one can still identify α and β spin-orbital "pairs" by the close similarity of their spatial distributions. In the spin-doublet 19-electron complexes examined here, one α spin-orbital has a spatial distribution with no β counterpart. This α spin-orbital is the one that we refer to as the SOMO. Because the SOMO in spin-doublet molecules has no counterpart of opposite spin, the SOMO dominates the spin density distribution. The EPR experiment is sensitive to the spin density, but experimentalists very often discuss their EPR results in terms of orbitals. More specifically, the amount of metal orbital character in the SOMO is of special interest in the EPR studies of 19-electron complexes. Because the spin densities calculated by DFT for the 19-electron complexes examined here are able to reproduce the experimentally observed EPR parameters, and because the calculated geometries are able to reproduce the ligand distortion or lack thereof, the orbitals from these calculations are appropriate for comparison to the orbitals that are based on discussions of EPR measurements.

The SOMO. Table 1 includes descriptions of the SOMO calculated by DFT for the three molecules described above. The contributions were calculated from the sum of the squares of the orbital coefficients for the atoms involved. This allowed direct comparison between the calculated results and those determined from the EPR measurements, where the magnitude of hyperfine coupling is approximately related to the orbital coefficients for the atom of interest.^{30,31}

The B3LYP results in Table 1 are chosen for discussion. The most important point to notice is that the metal atom orbitals in $\text{CpCr}(\text{CO})_2\text{NO}^-$, in which ligand distortion is most pronounced, still comprise a large percentage of the SOMO, about 30%, whereas the metal atom in $\text{CpW}(\text{NO})_2\text{P}(\text{OMe})_3$, in which there is no ligand distortion, contributes only half as much. The fact that the Cr–N–O bond in $\text{CpCr}(\text{CO})_2\text{NO}^-$ is significantly bent would lead some to categorize this molecule as an $18 + \delta$ complex because of the assumption that the ligand distortion implies strong localization of the unpaired electron on it. However, a comparison of the SOMOs of $\text{CpCr}(\text{CO})_2\text{NO}^-$ and $\text{CpW}(\text{NO})_2\text{P}(\text{OMe})_3$ in Table 1 shows that (1) distortion of a ligand does not necessarily imply low unpaired electron density on the metal and (2) the absence of ligand distortion does not imply high unpaired electron density on the metal or low density on the ligand. The bending of the Cr–N–O bond in $\text{CpCr}(\text{CO})_2\text{NO}^-$ is due to the fact that the Cr d_{xy} orbital interacts with the NO π^* orbital, and in order to improve bonding the Cr–N–O angle bends and the unpaired electron occupies an approximately sp^2 hybrid orbital on N. In $\text{CpW}(\text{NO})_2\text{P}(\text{OMe})_3$, none of the d orbitals on W contribute to the SOMO; therefore, no rehybridization at N occurs and the unpaired electron ends up in the π^* systems of the NO ligands.

Stability of $\text{CpMo}(\text{CO})_3\text{P}(\text{OMe})_3$. Because DFT methods have proved successful in modeling 19-electron compounds,^{6,7} we applied it to the hitherto unobserved

(27) Fängström, T.; Eriksson, L. A.; Lunell, S. *J. Phys. Chem. A* **1997**, *101*, 4814–4820.

(28) Qin, Y.; Wheeler, R. A. *J. Phys. Chem.* **1996**, *100*, 10554–10563.

(29) Duffy, N. W.; Nelson, R. R.; Richmond, M. G.; Rieger, A. L.; Rieger, P. H.; Robinson, B. H.; Tyler, D. R.; Wang, J. C.; Yang, K. *Inorg. Chem.* **1998**, *37*, 4849–4856.

(30) Atkins, P. W.; Symons, M. C. R. *The Structure of Inorganic Radicals*; Elsevier: Amsterdam, 1967.

(31) Symons, M. *Chemical and Biochemical Aspects of Electron-Spin Resonance Spectroscopy*; Wiley: New York, 1978.

molecule $\text{CpMo}(\text{CO})_3\text{P}(\text{OMe})_3$ to see whether this complex is stable toward dissociation of $\text{P}(\text{OMe})_3$. It was found that the 19-electron complex is only 0.8 kcal/mol higher in energy than $\text{CpMo}(\text{CO})_3$ plus $\text{P}(\text{OMe})_3$.³² This small barrier is consistent with the fact that an excess of phosphine is required for the production of $[\text{CpMo}(\text{CO})_3\text{P}(\text{OMe})_3]^+[\text{CpMo}(\text{CO})_3]^-$, whose formation is believed to result from electron transfer from $\text{CpMo}(\text{CO})_3\text{P}(\text{OMe})_3$ to $\text{Cp}_2\text{Mo}_2(\text{CO})_6$ followed by Mo–Mo bond homolysis in the latter.¹⁰ The small value of 0.8 kcal/mol is not quantitatively accurate at this level of theory, and the true value could be a few kcal/mol higher or lower. Qualitatively speaking, the calculated result indicates that there is only a small energy difference between the 19-electron complex and the 17-electron complex plus free $\text{P}(\text{OMe})_3$; thus, these species are in equilibrium.⁴

Conclusions

Density functional theory continues to be an excellent method for calculating the properties of organometallic compounds, and it has been invaluable in the study of species such as 19-electron complexes, which are often short-lived or difficult to isolate.^{6,7} The results of DFT calculations on $\text{CpCr}(\text{CO})_2\text{NO}^-$ and $\text{CpW}(\text{NO})_2\text{P}(\text{OMe})_3$ are in agreement with both the experimental geometries and EPR data, and it is therefore reasonable to make some conclusions about the electronic structure of these molecules. For $\text{CpCr}(\text{CO})_2\text{NO}^-$, it was found that the NO ligand bends significantly as a result of one-electron reduction of the 18-electron parent molecule. However, the Cr–N–O bond angle (157°) is larger than that

predicted by the analysis of the EPR data ($<130^\circ$), and the d orbitals of the chromium atom still make a significant contribution to the SOMO ($\sim 30\%$). DFT correctly predicts that the NO ligands are not significantly bent in $\text{CpW}(\text{NO})_2\text{P}(\text{OMe})_3$, which is consistent with the crystal structure of the closely related compound $\text{CpW}(\text{NO})_2\text{P}(\text{OPh})_3$. There is significant unpaired electron density on the NO ligands, however, and very little on the W atom. As expected, distortion of a ligand does imply localization of the unpaired electron on that ligand, but the fact that a ligand is not distorted does not necessarily mean that the unpaired electron has no appreciable amplitude on that ligand.

No Cp or $\text{P}(\text{OMe})_3$ ligand deformations occurred in either $\text{CpW}(\text{NO})_2\text{P}(\text{OMe})_3$ or $\text{CpMo}(\text{CO})_3\text{P}(\text{OMe})_3$. Calculations on $\text{CpCr}(\text{CO})_2\text{NO}^-$, $\text{CpW}(\text{NO})_2\text{P}(\text{OMe})_3$, $\text{CpMo}(\text{CO})_3\text{P}(\text{OMe})_3$, and $\text{CpCo}(\text{CO})_2^-$ showed that the cyclopentadienyl ring always accepts significant unpaired electron density, and it is therefore important in stabilizing 19-electron complexes.

$\text{CpMo}(\text{CO})_3\text{P}(\text{OMe})_3$ was shown to be very close in energy to $\text{CpMo}(\text{CO})_3 + \text{P}(\text{OMe})_3$. This result is consistent with the experimental requirement of using an excess of $\text{P}(\text{OMe})_3$ in the photochemical disproportionation reactions of $\text{Cp}_2\text{Mo}_2(\text{CO})_6$.²

Acknowledgment. This work was supported by the National Science Foundation and by the National Computational Science Alliance under Grant No. CHE990027N and utilized the NCSA HP-Convex Exemplar SPP-2000.

Supporting Information Available: A table of calculated bond lengths and angles for $\text{CpW}(\text{NO})_2\text{P}(\text{OMe})_3$ and experimental bond lengths and angles for $\text{CpW}(\text{NO})_2\text{P}(\text{OPh})_3$ (1 page). This material is available free of charge via the Internet at <http://pubs.acs.org>.

OM000261H

(32) The energy difference was corrected for the zero-point energies of the individual molecules but was not corrected for the effects of basis set superposition error.